Principles and potential of solvent gradient size-exclusion chromatography for polymer analysis

Niezen, L.E.; Kruijswijk, J.D.; van Henten, G.B.; Pirok, B.W.J.; Staal, B.B.P.; Radke, W.; Philipsen, H.J.A.; Somsen, G.W.; Schoenmakers, P.J.

DOI
10.1016/j.aca.2023.341041

Publication date
2023

Document Version
Final published version

Published in
Analytica Chimica Acta

License
CC BY

Analytica Chimica Acta 1253 (2023) 341041

Contents lists available at ScienceDirect

Analytica Chimica Acta

journal homepage: www.elsevier.com/locate/aca

Principles and potential of solvent gradient size-exclusion chromatography for polymer analysis

Leon E. Niezen [a,b,*,1], Jordy D. Kruijswijk [b,c,1], Gerben B. van Henten [a,b], Bob W.J. Pirok [a,b], Bastiaan B.P. Staal [d], Wolfgang Radke [e], Harry J.A. Philipsen [f], Govert W. Somsen [b,c], Peter J. Schoenmakers [a,b]

[a] Analytical-Chemistry Group, van 't Hoff Institute for Molecular Sciences, Faculty of Science, University of Amsterdam, Science Park 904, 1098 XH, Amsterdam, the Netherlands
[b] Centre for Analytical Sciences Amsterdam (CASA), the Netherlands
[c] Division of Bioanalytical Chemistry, Amsterdam Institute of Molecular and Life Sciences, Vrije Universiteit Amsterdam, Amsterdam, the Netherlands
[d] BASF SE, Carl-Bosch-Strasse 38, 67056, Ludwigshafen am Rhein, Germany
[e] PSS Polymer Standards Service, In der Dalheimer Wiese 5, 55120, Mainz, Germany
[f] DSM Engineering Materials, Urmonderbaan 22, 6167 RD, Geleen, the Netherlands

HIGHLIGHTS

- Principles and applications of gradient size-exclusion chromatography were studied.
- The method can be used to determine the polymer chemical composition distribution.
- It can be a useful alternative to conventional reversed-phase liquid chromatography.
- "Breakthrough" phenomena, present in conventional methods, are avoided.
- The technique may be especially useful as a second-dimension separation in LC × LC.

GRAPHICAL ABSTRACT

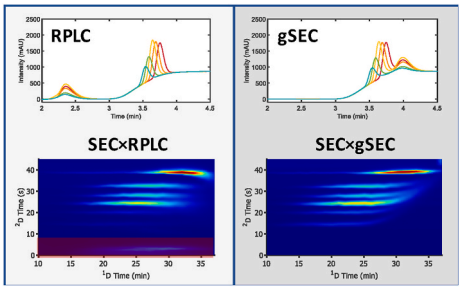

ARTICLE INFO

Handling Editor: Prof. W.W. Buchberger

Keywords:
SEC-Gradients
Gradient-elution liquid chromatography
Size-exclusion chromatography
Polymer analysis
Breakthrough
Chemical composition

ABSTRACT

The properties of a polymeric material are influenced by its underlying molecular distributions, including the molecular-weight (MWD), chemical-composition (CCD), and/or block-length (BLD) distributions. Gradient-elution liquid chromatography (LC) is commonly used to determine the CCD. Due to the limited solubility of polymers, samples are often dissolved in strong solvents. Upon injection of the sample, such solvents may lead to broadened or poorly shaped peaks and, in unfavourable cases, to "breakthrough" phenomena, where a part of the sample travels through the column unretained. To remedy this, a technique called size-exclusion-chromatography gradients or gradient size-exclusion chromatography (gSEC) was developed in 2011. In this work, we aim to further explore the potential of gSEC for the analysis of the CCD, also in comparison with conventional gradient-elution reversed-phase LC, which in this work corresponded to gradient-elution reversed-phase liquid chromatography (RPLC). The influence of the mobile-phase composition, the pore size of the stationary-phase particles, and the column temperature were investigated. The separation of five styrene/ethyl

* Corresponding author. Postbus 94157, 1090 GD, Amsterdam, the Netherlands.
E-mail address: L.E.Niezen@uva.nl (L.E. Niezen).
[1] Equal contribution.

https://doi.org/10.1016/j.aca.2023.341041
Received 14 December 2022; Received in revised form 1 March 2023; Accepted 2 March 2023
Available online 4 March 2023

acrylate copolymers was studied with one-dimensional RPLC and gSEC. RPLC was shown to lead to a more-accurate CCD in shorter analysis time. The separation of five styrene/methyl methacrylate copolymers was also explored using comprehensive two-dimensional (2D) LC involving gSEC, *i.e.* SEC × gSEC and SEC × RPLC. In 2D-LC, the use of gSEC was especially advantageous as no breakthrough could occur.

1. Introduction

Polymers are among the most important building blocks of materials. The applications of polymers are nearly limitless, from packaging applications to electronics, paints, clothing, and drug delivery systems. To continuously improve polymeric materials, it is vital to understand how their molecular structure and composition relate to their physical properties. Several techniques can be used to characterize the chemical structure of polymers, including pyrolysis – gas chromatography coupled to mass spectrometry, and spectroscopic methods such as infrared, ultraviolet absorbance, Raman or nuclear magnetic resonance spectroscopy [1–6]. However, most of these methods merely provide average polymer composition, and do not yield information on the distributions present, such as molecular-weight (MWD), chemical-composition (CCD), and/or block-length (BLD) distributions. To assess these distributions, liquid chromatography (LC) is more generally used [7–16]. A common LC technique for the analysis of polymers is size-exclusion chromatography (SEC), which is a well-established benchmark for determining molecular-weight distributions (MWD) [1,10,13,14]. There is no such benchmark method for the analysis of the CCD, although gradient-elution LC is probably most commonly used [7–11,15,16].

The greatest challenges for the application of solvent-gradient LC are analyte detection and polymer solubility. Due to the changing mobile-phase composition, many typical detectors used for SEC, such as refractive-index, viscometric, or light-scattering detectors cannot be used. Efforts to make such detectors work with gradients [17–20] have been moderately successful at best. Many polymers are difficult to dissolve. Strong solvents and patience are typically required and injecting the resulting sample at the starting conditions of a gradient separation, in a weak eluent, can be problematic. This may be exacerbated for crystalline (co)polymers, due to issues with slow redissolution [21]. Even if crystallinity is not an issue, a sample solvent that is a strong eluent can still lead to broad or deformed peaks and, ultimately, to a phenomenon called breakthrough [22]. When this occurs a part of the sample stays in the solvent plug and passes (nearly) unretained through the column. Several methods have been developed to address this issue [23,24]. These include sandwich injection [23] and solvent-mixing strategies [24]. Additionally, so-called barrier methods may be applied [25,26]. However, the latter fundamentally result in very low peak capacities (one per barrier). SEC-gradients, henceforth referred to in this work as gradient-SEC (gSEC), can be seen as a much-improved implementation of a barrier method, with a gradual rather than stepwise change in mobile-phase composition. Originally introduced by Schollenberger et al. [27,28], gSEC eliminates the risk of breakthrough and offers a much larger peak capacity than conventional barrier methods (the principles and practise of gSEC are outlined below). However, reports on the use of gSEC for the separation of synthetic polymers have so far been scarce [27–30]. While some work has been performed illustrating different elution mechanisms [27,28], many aspects of gSEC have not yet been studied. These include the influence of the solvent composition and of the column packing material (*e.g.* the particle pore size). Importantly, gSEC has never been directly compared with conventional gradient-elution LC, neither in one-dimensional LC nor as a second-dimension separation in two-dimensional LC.

Our objectives in the present work were to critically evaluate the influence of the mobile phase, the temperature, and the pore size in gSEC, and to compare RPLC and gSEC, so as to highlight the advantages and shortcomings of both methods. SEC separations of polystyrene (PS) and polymethyl methacrylate (PMMA) were performed on various columns of different chemistries, containing particles of different pore sizes, and using various mobile-phase mixtures of acetonitrile (ACN) and tetrahydrofuran (THF), at two different temperatures (25 and 60 °C). Following these experiments, gSEC measurements were performed using small-pore stationary-phase particles. We set out to compare the separation of five styrene/ethyl acrylate (S/EA) copolymers and five styrene/methyl methacrylate (S/MMA) copolymers, each characterized by a broad MWD, but a narrow CCD. Both RPLC and gSEC were used for the separation of the S/EA copolymers. For the S/MMA copolymers comprehensive two-dimensional liquid chromatography (LC × LC) in either SEC × RPLC or SEC × gSEC mode were applied. To perform SEC × RPLC successfully, we needed to avoid breakthrough in the second dimension. This is notoriously difficult, because a strong first-dimension solvent is combined with a large second-dimension injection volume. In SEC × gSEC breakthrough did not occur, as the strong first-dimension solvent matches the starting conditions of the gSEC separation.

2. Theory

The retention of an analyte may be described using the retention factor (k), given by

$$k = \frac{t_R - t_0}{t_0} \tag{1}$$

where t_R is the retention time of the analyte and t_0 is the void time of the column (given by the void volume V_0, divided by the flowrate, F), or the time it takes for an unretained marker to move through the column. On a particular column, k is commonly adjusted by changing the mobile phase composition and/or the temperature. Solvents are generally classified as either weak (causing large k) or strong (causing small k). For a polymer, solubility will also play a role and an eluent can be either a solvent or a non-solvent. Only when a polymer is soluble will the eluotropic strength affect the separation. For high-molecular-weight analytes, such as polymers, the size (hydrodynamic radius) of the analyte molecules in relation with the pore diameter of the packing material also plays a role for retention. When the solvent strength is sufficiently high, no interaction occurs between the analytes and the packing material. The elution order is then (ideally) determined solely by the hydrodynamic volume of the polymer, as the accessible pore volume will be different for polymers of different sizes (size-exclusion conditions). In this case, elution occurs before t_0 and the analytes travel faster than the surrounding mobile phase. On the other hand, at low solvent strength k may be very large, in which case, the polymer will not elute from the column. When increasing the fraction of strong solvent (φ) in the case of gradient elution, retention (*i.e.* the local retention factor) decreases with time. The migration of the polymer through the column now depends on how quickly k decreases with φ. If there is no interaction with the column at the mobile phase composition where the polymer is first soluble, the elution composition will be solely determined by the polymer's solubility [12,31], which will depend on the polymer's molecular weight and its chemical composition. In all other cases the polymer will elute "normally", *i.e.* primarily based on the strength of interaction with the column material [32–34]. The observed effect of polymer exclusion from the pores of the stationary phase will be significantly smaller, because as soon as polymer molecules move faster than the mobile phase they will experience a weaker solvent and be retained again until the eluent strength is sufficient.

To describe the gradient-elution process quantitatively it must be

known how φ changes with time, and how k changes with φ. In previous work, it has been shown that the retention of a polymer in gradient-elution RPLC is reasonably well described by a log-linear model, often referred to as the linear-solvent strength (LSS) model [32–36]. It is assumed that the logarithm or natural logarithm of the retention factor (k), varies linearly with φ. Based on this model an "effective" gradient steepness parameter can be defined. Using this concept, it was shown that effectively steep gradients minimize the influence of the MWD on retention, while the influence of the CCD is enhanced [37]. In such a steep gradient all molecules of a specific homopolymer, or of a co-polymer of a given composition, are found to elute at a specific ("critical") composition (φ_{crit}), independent of their molecular weight [33,34,37–43].

Effectively steep gradients are most easily realized by using a step gradient, changing instantaneously from an initial composition (φ_{init}, weak eluent, high k) to a final composition (φ_{final}, strong eluent, low k) higher than φ_{crit}. However, this results in co-elution of all analytes (homopolymers and copolymers) with critical compositions that fall within the range of φ that is covered by the gradient (*i.e.* $\varphi_{init} \leq \varphi_{crit} \leq \varphi_{final}$). This implies that a finite $\Delta\varphi$ results in co-elution of a (large) faction of the CCD of a copolymer. Therefore, a step gradient cannot be used to determine the CCD. For this purpose, a continuous gradient must be used, of which linear gradients are most common. However, a step gradient may be used to separate two different homo- or co-polymers with sufficiently different φ_{crit}.

Normally, analytes are injected before the gradient arrives at the column inlet. It is also possible to inject the analyte after the end of the step gradient has passed the injector. If $\varphi_{crit} \leq \varphi_{final}$, the injected analyte molecules experience SEC conditions, and large molecules travel through the column faster than the gradient. This results in so-called "barrier" methods, where a step gradient ($\varphi_{init} \leq \varphi_{crit} \leq \varphi_{final}$) is established within the column before injection [25,26]. If the analyte travels much faster than the solvent and the time of injection is not too far after the step gradient has passed the injector, the analyte molecules may catch up with the gradient step. They cannot move past the gradient, as they would experience a weaker solvent and slow down. Again, all analytes with $\varphi_{init} \leq \varphi_{crit} \leq \varphi_{final}$ will co-elute at the moment the step gradient reaches the end of the column. Once again, the use of a continuous (*e.g.* a linear) gradient, from a weak solvent to a strong solvent, will provide a better characterization of the CCD. This latter type of method is referred to as gSEC [27–30].

As with conventional gradient-elution RPLC, a gSEC separation that is based primarily on the CCD is desirable. Such a separation can be combined with SEC to achieve high orthogonality in LC × LC. With a conventional gradient, the influence of the MWD is reduced when using effectively steep gradients [37]. In the case of gSEC this is also true. Whether analyte molecules can reach φ_{crit} before the gradient elutes from the column depends on two factors. Namely, the extent of exclusion the analytes experience, and on how far they must travel through the column to reach φ_{crit}.As with a conventional gradient, the effective gradient steepness depends on the ratio of the column volume to the gradient volume. At constant column volume, a smaller gradient volume (steeper gradient) implies that the analyte has to travel less far to reach φ_{crit}. A larger column volume (relative to the volume of the gradient) implies that analyte molecules have a greater chance (*i.e.* a greater part of the column) to reach φ_{crit}. The maximum gradient volume ($V_{G,max}$), such that analyte molecules can reach φ_{crit}, can be calculated if a set of criteria are met, *viz.* (*i*) a critical composition exists for a particular combination of mobile phase, stationary phase, and analyte (*i.e.* $\varphi_{init} \leq \varphi_{crit} \leq \varphi_{final}$, where the initial and final compositions may cover the entire range from 0 to 1), (*ii*) the analyte molecules are unretained at $\varphi > \varphi_{crit}$, (*iii*) the injection takes place at the moment the end of the gradient arrives at the column inlet, and (*iv*) the calibration curve for the column is known. $V_{G,max}$ may then be calculated using

$$V_{G,max} = \frac{V_0 - (V_i + K_{SEC}V_p)}{1 - \frac{\varphi_{crit} - \varphi_{init}}{\varphi_{final} - \varphi_{init}}} = \frac{\Delta\varphi}{\varphi_{final} - \varphi_{crit}}(V_0 - (V_i + K_{SEC}V_p)) \quad (2)$$

where V_i and V_p are the interstitial, and pore volume, respectively, and K_{SEC} is the SEC distribution coefficient. It is assumed that $V_0 = V_i + V_p$. Note that any smaller gradient volume would lead to a steeper gradient and causes elution of the analyte at $\varphi = \varphi_{crit}$; hence, our use of the term "maximum gradient volume". For gradient volumes larger than $V_{G,max}$ the analytes cannot catch up with φ_{crit} and elute unretained. In such situations, elution is based on hydrodynamic size, but not on chemical composition. In gSEC, each analyte will have to first move some distance through the column to reach φ_{crit}. This is in contrast with conventional gradient-elution LC, where migration of the analyte polymers will, for relatively large molecular-weight analytes, occur within the vicinity of φ_{crit} as the analyte is first retained at the head of the column. As a result, a steeper gradient will be required using gSEC compared to conventional gradient-elution LC to separate high-molecular-weight polymers with different φ_{crit}. Some other general conclusions can also be drawn from Equation (2), namely: *i*) to avoid the use of very small gradient volumes, analyte exclusion should be promoted (K_{SEC} should be minimized) by choosing small-pore-size packings, *ii*) columns with a large pore volume (V_p) are preferred, since this maximizes the migration velocity of the analyte relative to the mobile-phase velocity, and *iii*) V_G will be determined by the polymer with the smallest φ_{crit} in the sample. Under the assumptions underlying Equation (2), it is clear that gSEC will perform better when the difference between φ_{crit} and φ_{final} is reduced. However, this would hinder the ability of the method to analyse samples of widely different chemical composition, since these samples will feature large differences in φ_{crit}. Once again, conventional gradient-elution will be less affected by this, since analytes will only move within the vicinity of φ_{crit}. In this study we set out to evaluate the points raised above and to verify the conclusions drawn from Equation (2).

3. Experimental

Two different systems (A and B), in two different laboratories (referred to below as laboratory A, located at the University of Amsterdam and laboratory B, located at the Vrije Universiteit Amsterdam), were used for different parts of this work. Certain samples were common to both laboratories, these are described here.

A polystyrene (PS) standards kit was obtained from PSS (Mainz, Germany) and polymethylmethacrylate (PMMA) standards were obtained from Polymer Laboratories (Church Stretton, UK). Styrene/methyl methacrylate (S/MMA) and styrene/ethyl acrylate (S/EA) co-polymers were synthesized in-house using thermally initiated free-radical polymerization, the procedure, chemicals, along with their molar masses, polydispersity, and approximate average chemical composition are included in the supplementary information (Tables S–1, Section S-1).

3.1. Laboratory A

3.1.1. Chemicals and materials

Non-stabilized tetrahydrofuran (THF, 99.9%, LC-MS Grade) and toluene (99%, LC-MS grade) were obtained from VWR Chemicals (Darmstadt, Germany), acetonitrile (ACN, ≥99.9%, LC-MS Grade) was obtained from Biosolve (Valkenswaard, The Netherlands).

3.1.2. Systems and equipment

The experiments in this study were carried out on an Agilent system, combining components from both an Agilent 1100 and a 1290 Infinity 2D-LC system, all obtained from Agilent (Waldbronn, Germany). The system included an 1100 autosampler (G1313A), an 1100 capillary pump (G1376A), a 1290 binary pump (G7120A) equipped with a jet weaver V35 mixer, and a 1290 column compartment (G1316C)

equipped with a 2-position/8-port valve (model 5067–4214). For detection, the system comprised a 1290 diode-array detector (DAD, G4214A) with a max-light cartridge cell (model G4212-6008, 10 mm path length, 1 μL cell volume), and a 1260 evaporative light-scattering detector (ELSD, G4260B). The capillary pump was used for the ^{1}D SEC measurements and the binary pump for the gSEC experiments. The system was controlled using Agilent OpenLAB CDS ChemStation software (rev. c.01.10).

The ^{1}D-gSEC and SEC-recovery experiments were carried out on an Agilent 1290 Infinity LC system. This system included a 1290 Infinity II autosampler (G7129B), a 1290 binary pump (G7120A) equipped with a jet weaver V35 mixer, and a 1290 MCT column oven (G7116B). For detection, the system comprised a 1290 DAD (G7117B) with a max-light cartridge cell (Model G4212-6008, 10 mm path length, 1 μL cell volume). The system was controlled using Agilent OpenLAB CDS ChemStation software (rev. c.01.10).

Conventional (isocratic) SEC measurements were performed at various ACN/THF eluent compositions, at 25 and 60 °C. The flow rate was 0.5 mL•min^{-1}, the injection volume 3.0 μL, and the sample concentration was 0.5 mg•mL^{-1}. Columns used for these experiments included a 50 × 4.6 mm XBridge bridged ethylene hybrid (BEH) Shield RP18 XP column, packed with 130 Å, 3.5-μm particles, two Nova-Pak 150 × 3.9 mm C18 columns packed with 60 Å, 4-μm particles, all purchased from Waters (Milford, MA, USA), as well as a 150 × 4.6 mm Dionex Acclaim Polar-Advantage C18 column packed with 300 Å, 3-μm particles purchased from Dionex (Sunnyvale, CA, USA), and two sets of two 250 × 4.6 mm Nucleosil columns (C_{18} and bare silica), both packed with 4000 Å, 5-μm particles, purchased from Macherey Nagel (Düren, Germany).

For the 1D-LC gSEC experiments, three different silica-based C_{18} columns were used; often multiple columns of the same type were coupled in series. These columns included two 50 × 4.6 mm and one 100 × 4.6 mm XBridge BEH Shield RP18 XP columns, packed with 130 Å, 3.5-μm particles, the two Novapak columns, and the Dionex Acclaim Polar-Advantage C_{18} column. For these experiments an injector program was used to realize the required delayed injection. Injection was timed to occur 1 min after the start of the experiment, *i.e.* at the end of the gradient. A variable initial hold-up time was programmed into the gradient so that gradient volumes could be varied based on the volume of each column, while simultaneously keeping the injection time constant. The measured retention times were not adjusted for the injection time and are relative to the start of the experiment.

For the 2D-LC experiments, two 150 × 2.1 mm APC SEC columns packed with 2.5-μm BEH particles with 450 Å pore size were used in the first dimension, while for the second-dimension separation two of the 50 × 4.6 mm XBridge BEH Shield RP18 XP columns were used. All columns were obtained from Waters. For SEC × RPLC, the gradient program was as follows: 0–0.1 min linear gradient 80/20% ACN/THF, 0.1–0.65 min linear gradient 50/50%, 0.65–0.75 linear gradient 45/55%. For SEC × gSEC, it was the following: 0–0.1 min isocratic 40/60% ACN/THF, 0.1–0.2 min linear gradient to 95/5%, 0.2–0.35 min linear gradient 20/80%, 0.35–0.9 min linear gradient 50/50%, 0.9–0.95 min linear gradient 45/55%, 0.95 min isocratic 40/60%.

The data of φ_{crit} *vs.* temperature for polystyrene (included in the supplementary information) was obtained from gradient experiments performed at different temperatures on the XBridge column. The approximate critical composition at each temperature was determined based on the approach described by Fitzpatrick et al. [34] using gradients from 0 to 60% THF in ACN in 5, 10, 15, 20 and 25 min, at a flowrate of 0.5 mL•min^{-1}.

Data analysis was performed in MATLAB R2020a (Mathworks, Woodshole, MA, USA).

3.2. Laboratory B

3.2.1. Chemicals and materials

Acetonitrile (ACN, ≥99.9%, HPLC Grade) was obtained from Biosolve, non-stabilized tetrahydrofuran (THF, HPLC grade) was obtained from VWR Chemicals.

3.2.2. Systems and equipment

The experiments were performed on a 1290 Infinity II Agilent system. The system included an autosampler (G7167B), a quaternary pump (G7104A), a multi-column thermostat (MCT, G7116B). A variable-wavelength detector (VWD, G7114B) and an ELSD (G7102A) were used for detection. The VWD was set to record UV absorption at 210 and 260 nm.

Conventional (isocratic) SEC measurements were performed at various ACN/THF eluent compositions, at 25 and 60 °C. The flow rate was 0.5 mL•min^{-1}, the injection volume 3.0 μL, and the sample concentration was 0.5 mg•mL^{-1}. Columns used for these experiments were all Zorbax columns purchased from Agilent. These included a 100 × 4.6 mm Rapid Resolution StableBond C_{18} column, packed with 300 Å, 3.5-μm particles, a 250 × 9.4 mm semi-preparative StableBond C_{18} column packed with 300 Å, 5-μm particles, and a 250 × 9.4 mm semi-preparative StableBond C_{18} column packed with 80 Å, 5-μm particles.

For the ^{1}D-gSEC and RPLC experiments in sections 4.3 and 4.4, the gradient program is described in the respective figures. The temperature was 25 °C, the flow rate 0.5 mL•min^{-1}, the injection volume 3.0 μL, and the sample concentration 0.5 mg•mL^{-1}. Once again, a delayed injection was used for the gSEC experiments. The injection took place after a delay of 0.4 mL (48 s) to account for the system dwell volume. These experiments were carried out on Rapid Resolution StableBond column.

4. Results and discussion

4.1. Influence of mobile-phase composition on elution volume in SEC

The elution volume in SEC is generally thought to be independent of the nature and composition of the solvent, provided that interactions with the stationary phase are absent. However, the size (hydrodynamic radius) of molecules in solution may be affected by the nature of the solvent. Because the solvent composition is varied in gSEC, it is relevant to investigate the effects of solvent composition on elution volumes and calibration curves in SEC. Similar work, albeit using overall stronger mobile phase compositions, has previously been performed by Caltabiano et al. [44].

Conventional (isocratic) SEC experiments were performed using different fractions of THF in ACN, all of which were above the φ_{crit} of PS and PMMA (expected $\varphi_{crit,PMMA} \approx 0.09 - 0.10$ *vs.* $\varphi_{crit,PS} \approx 0.5$), to ensure SEC behaviour. The results of these SEC experiments for homopolymer PS and PMMA on various columns with different pore sizes and chemistries are provided in Fig. 1.

The elution volume of PS increases with an increase of the concentration of weak solvent (ACN) on all C_{18} stationary phases, whereas the effect of the THF fraction on the elution volume of PS is small on the one bare-silica column tested (Fig. 1-H). The possible explanations for the increase in elution volume with a decrease in strong solvent when using the C_{18} columns include the following.

i) the polymeric coil size/hydrodynamic volume decreases with an increase of the weak solvent. This effect should be independent of the column used;
ii) the pore volume of the column changes with the mobile phase composition, due to a swelling or shrinking of the packing particles;
iii) non-SEC interactions occur with the stationary phase as the mobile-phase composition approaches φ_{crit};

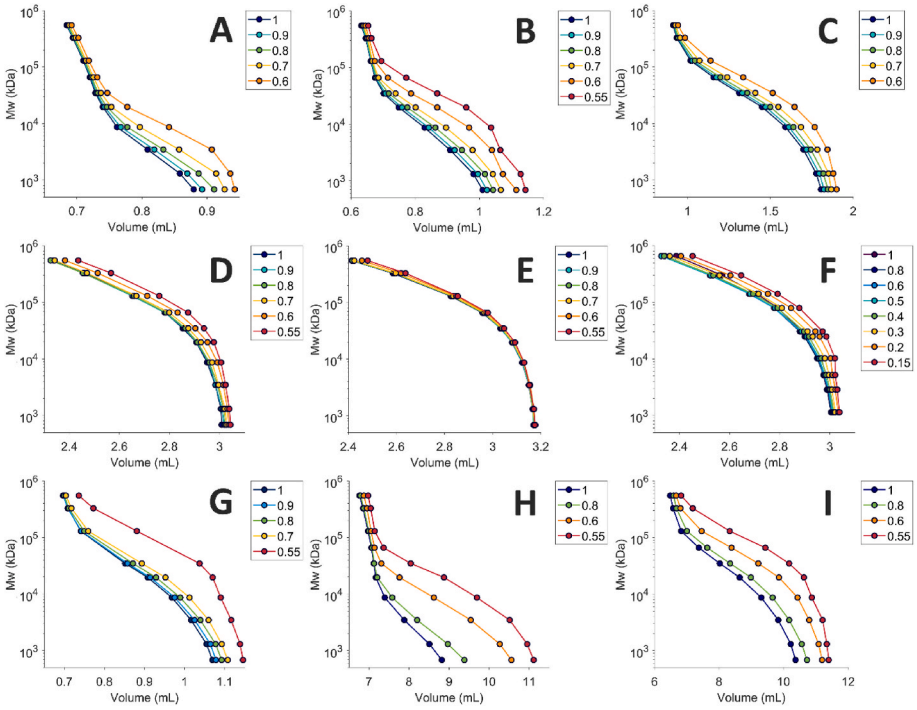

Fig. 1. SEC calibration curves of ten PS standards (A–G) and ten PMMA standards (H–I) obtained for different mobile phase compositions at 25 °C. The fraction of THF (in ACN) is indicated in the legend. Columns: A) Novapak C18 (150 × 3.9 mm, 60 Å), B) Two XBridge C18 (50 × 4.6 mm, 130 Å), C) Dionex C18 (150 × 4.6 mm, 300 Å), D and I) Nucleosil C18 (250 × 4.6 mm, 4000 Å), E), Zorbax SB C18 (100 × 4.6 mm, 300 Å), F) Zorbax SB C18 (250 × 9.4 mm, 80 Å), G) Zorbax SB C18 (250 × 9.4 mm, 300 Å), and H) Nucleosil Bare Silica (250 × 4.6 mm, 4000 Å).

iv) a change in the ratio of the interstitial to pore volume occurs due to a change in the thickness of the C_{18} layer with mobile-phase composition.

Several of these effects may occur concomitantly. Explanation (*i*), the addition of ACN (non-solvent for PS) is expected to result in a contraction of the PS chain. Precipitation of PS occurs at a composition of about 50% ACN in THF. For the bare silica columns (Fig. 1-H) ACN is a stronger (more polar) solvent than THF. However, because both solvents are strong, retention on these columns should not be strongly affected by the ratio of ACN/THF. Thus, the small increase in elution volume observed for the larger standards on the bare silica column might be mainly attributed to the change of coil size with eluent composition. The effect should increase with increasing polymer size and be most prominent in the linear (shallow) part of the calibration curve. This is indeed observed in Fig. 1-F. For similar slopes of the calibration curves this effect is expected to occur to similar extend also on C_{18} columns, but there it is likely overshadowed by other effects.

Explanation (*ii*), an effect of the mobile-phase composition on the volume occupied by the solid packing material in the column is considered highly unlikely for the silica particles used in the present study. The effect may be quite significant when other types of particles, such as PS cross-linked with divinylbenzene (PS-DVB), are used.

This leaves an increase in interaction of the analyte molecules with the C_{18} layer (Explanation *iii*) or a change in the stationary phase volume (Explanation *iv*) as the more-probable causes of the significant increase in elution volume on the C_{18} columns. Explanation *iii* is an analyte-specific effect, whereas Explanation *iv* is column specific. Therefore, it may be possible to distinguish between the two effects by performing the same experiments with a series of analyte polymers with similar hydrodynamic volumes, but a different chemical structure. Hence, the experiments on the 4000 Å Nucleosil C18 column (Fig. 1-D) were repeated for a set of PMMA standards (Fig. 1-I). At first sight, the observed variations in the calibration curves seem to be similar for the PS and PMMA standards. However, a closer inspection of the data reveals that at low concentrations of ACN the elution volume of the PMMA standards slightly increases with an increase in ACN content, whereas an increase in elution volume is observed at high concentrations of ACN. The maximum effect for PMMA is reached at 85% ACN in Fig. 1-I, whereas in the case of PS it is already reached at 45% ACN (see supplementary information, Figure S-1, section S-2). For both PS and PMMA it seems that the effect is strongest when the mobile-phase composition is close to φ_{crit}. Clearly, the observed effects depend on the analyte polymer, which is a strong indicator that interactions with the stationary phase (Explanation *iii*) account for the largest changes in elution volume, with changes in C_{18} layer thickness (Explanation *iv*) and polymer hydrodynamic volume (Explanation *i*) playing secondary roles. The same conclusions can be drawn from experiments with PMMA on the columns used in Fig. 1-E/F/G (see supplementary information, Figure S-2, section S-2).

If the elution volume increases because of retention, then it should be possible to estimate φ_{crit} by fitting a retention model to the elution volume *vs.* φ data for the analyte polymers of various molecular weights. According to the LSS model, the changes in elution volume can be fitted to an exponential equation for analytes that show reasonably large changes with φ (*e.g.* those that elute in the linear part of the calibration curve). The intersection point of the fitted lines for analytes of different molar mass should correspond to a reasonable estimate for φ_{crit} [33,34,37]. This approach was performed for the data in Fig. 1-A/B/C. However, $t_R < t_0$, k is negative (and hence ln k undefined) for our data. In that case, it is not possible to use the LSS model. Instead, we chose to fit a different equation ($V_e = k_0 e^{-S\varphi} - c$). Here, k_0 and S still correspond to k at $\varphi = 0$ and the change in k with φ, respectively. The third parameter, c, accounts for a reduction in V_0 with molecular weight, due to the limited accessibility of the pore volume. Fitting this equation only gave a reasonable estimate for $\varphi_{crit,PS}$ (approximately 50%) on the XBridge column (Fig. 1-B). This may be because the analyte's interaction with the column is (likely) very weak when the mobile phase composition is stronger than φ_{crit}. The effect of a change in analyte hydrodynamic volume with φ is then also relatively enhanced. Both effects will complicate the extrapolation that is required to determine φ_{crit}, implying that measurements must be performed close to the critical composition to yield good estimates of φ_{crit}, which means such predictions are not very useful.

Similar experiments, as those underlying Fig. 1, were also performed at a temperature of 60 °C for some of the columns (supplementary

information, Figure S-3, section S-2). Compared to 25 °C, a shift towards a lower elution volume was observed for all analytes (including the t_0 marker, toluene) and columns. Based on the thermal expansion coefficients of ACN and THF this shift is likely a result of a thermal expansion of the mobile phase (from the pump temperature to the column temperature) and the concomitant increase in velocity. Apart from this general shift, at higher temperatures the variation of the elution volume with mobile-phase composition is seen to be smaller. This is consistent with the above explanation, as a higher temperature generally leads to a reduction in enthalpic interactions. Moreover, in the present system an increased temperature leads to a shift of φ_{crit} to lower φ, implying that the experiments across the same range of φ are performed further from φ_{crit}, and, hence, the increase in elution volume will be smaller at higher temperatures (supplementary information, Figure S-4, section S-2).

One aspect that has not been discussed is the diminishing effect of the solvent composition for analyte polymers that approach the exclusion limit of the column (see for example Fig. 1-A). Two competing effects determine the overall variation observed. Larger molecules are expected to exhibit greater interaction with the column, because in adsorption or partition LC retention increases exponentially with molecular weight [33,34]. The opposing effect is a reduction in available surface area for larger polymers, which depends on the ratio of the size of the polymer in solution (hydrodynamic radius) and the pore-size distribution of the packing material. The result of the two competing effects may be that the effect of mobile phase composition is largest for analytes eluting within the most-selective range of the calibration curve. When comparing different columns, it is seen that an increase in pore size (see for example Fig. 1-D) results in an increase in the effect of φ on the high-molecular-weight analytes, as these are no longer fully excluded. For low-molecular-weight polymers ($M_w \approx 10^3$ Da) the effect of composition is much greater in Fig. 1-A than in Fig. 1-D. Such analytes fully permeate all pores in the latter case. However, the total available surface area is much smaller on the 4000 Å column used to record Fig. 1-D than on the 60 Å column used to record Fig. 1-A.

Irrespective of the cause of a change in elution volume, the above results imply that Equation (2) only provides an approximate value for the required gradient steepness in case of gSEC when C_{18} columns are used. Any shifts towards higher elution volumes (*i.e.* less exclusion) implies that steeper gradients than predicted by Equation (2) will be required in gSEC to achieve a separation dominated by the CCD. While in principle it should be possible to estimate the required gradient steepness based on experiments where the slope of the gradient is varied, this will be challenging because the change in retention with gradient steepness is likely too small in gSEC. Hence, this was not investigated.

4.2. Influence of pore size in gSEC

To investigate the influence of the pore size in gSEC, the separation of a series of polystyrenes was performed using several different columns (Fig. 2). The standard deviation of the elution time, as determined from triplicate measurements was, in nearly all cases, below 0.002 min.

Fig. 2 shows that for all columns the elution time still varies with analyte molecular weight. Although the elution time differences are small, these variations are consistent and significant. Under the applied conditions, it was not possible to achieve a fully molecular-weight-independent elution on any of the columns. This was quite disappointing, considering that the difference between the eluent composition at the injection point (φ_{final}) and the approximate φ_{crit}, as determined from earlier gradient-elution LC experiments of large standards, was only about 0.1. This difference corresponds to only about 5–7% of the column volume, depending on the exact column used. Apparently, to achieve molecular-weight-independent elution, even steeper gradients would be required. On the column with the smallest pores (Fig. 2-A), an inversion of the molecular-weight dependence of the elution time can be observed for the highest molecular-weight

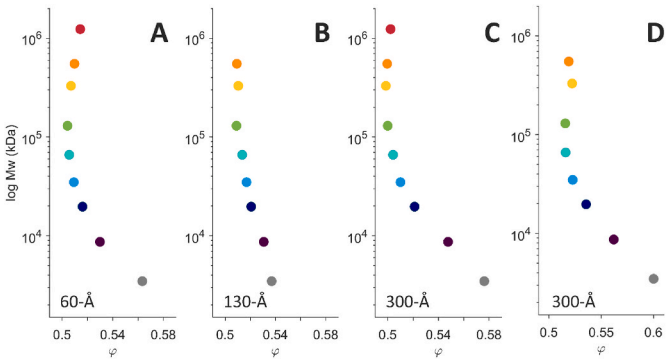

Fig. 2. Approximate elution composition of PS standards of different molecular weight in gSEC on four different columns. The column oven temperature was set to 25 °C. Linear gradient from 5 to 60% THF in ACN; the gradient duration (t_G) and flowrate were adjusted based on the column. Injection was timed to occur at the end of the gradient. A) Two Novapak columns (150 × 3.9 mm, 60 Å; $t_G = 0.50$ min, flow: 1.0 mL•min^{-1}, $V_G/V_0 \cong 0.30$); B) Two XBridge columns (50 × 4.6 mm, 130 Å; $t_G = 0.80$ min, flow: 0.5 mL•min^{-1}, $V_G/V_0 \cong 0.40$); C) Dionex column (150 × 4.6 mm, 300 Å; $t_G = 0.65$ min, flow: 0.9 mL•min^{-1}, $V_G/V_0 \cong 0.35$); D) Zorbax column (100 × 4.6 mm, 300 Å; $t_G = 0.65$ min, flow: 0.5 mL•min^{-1}, $V_G/V_0 \cong 0.30$).

standards. Confounding SEC and interaction-LC mechanisms, or potentially confounding interaction and precipitation effects, probably prohibit genuine critical behaviour. For the different columns, a loss in recovery was also observed for specific standards (supplementary information, Tables S–2, section S-3). For the 60 Å columns, low recoveries of 11% and 19% were obtained for the standards of 130 and 330 kDa, respectively. The largest standards (552 and 1270 kDa) showed higher recoveries (80–90%, or higher). On the 130 Å column, the standards of 330 and 552 kDa showed low recoveries (11% and 7%, respectively). For the 300 Å column (Dionex), the loss in recovery was significantly smaller, with 79% as the lowest recovery for the 330 kDa standard. The loss in recovery seems related to the pore size of the stationary phase particles. Possibly, as a result of small changes in hydrodynamic volume with mobile-phase composition, analytes may get trapped when their size is similar to the pore. This explanation is supported by the data and discussion of Fig. 1, and will be especially important to consider for the quantitation of copolymers that feature a broad MWD. The very fast gradients applied in gSEC may give rise to differences in mobile-phase composition within and outside the pores. Small analytes have ample room to move in and out of the pores, whereas the largest analytes do not enter the pores at all. Since in gSEC the gradient must always pass through the column before the analytes, insufficient equilibration in small pores is difficult to avoid. In columns with larger pores (and smaller surface areas), column equilibration will be faster and differences in eluent composition in and outside the particles will be smaller [45]. However, such columns will diminish the extent of exclusion, and, consequently, steeper gradients will be required to attain elution independent of molecular weight.

4.3. Influence of gradient steepness

To further investigate the effects of the gradient steepness on elution behaviour and recovery, a series of PMMA and PS standards were subjected to different gradient volumes on the Zorbax 300 Å column. In Fig. 3, the influence of gradient steepness is illustrated for PS and PMMA standards when analysed with both gSEC and RPLC.

For the gSEC experiments (Fig. 3, open markers), an increase in gradient steepness (moving from Fig. 3-A to C) did result in the expected decrease in molecular-weight dependence for both the PS and PMMA standards. Note that retention times are relative to the experiment start and not relative to the injection time. However, for the PMMA standards, which must travel significantly further through the gradient to

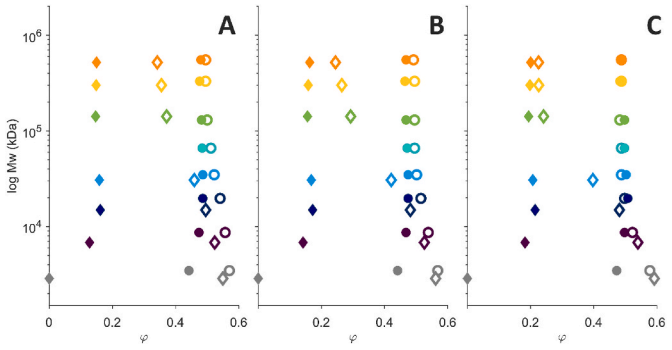

Fig. 3. Approximate elution composition of different (known) molecular weight PS (circles) and PMMA (diamonds) standards in gSEC (open markers) and RPLC (filled markers) obtained at different gradient steepnesses using the Zorbax (4.6 × 100 mm), 300 Å column. In all cases, a linear gradient from 0 to 60% THF in ACN was used at a flow of 0.5 mL•min^{-1}. The column oven temperature was set to 25 °C. The gradient duration was varied as follows: A) 2.0 min ($V_G = 1$ mL, $V_G/V_0 \cong 0.83$), B) 1.2 min ($V_G = 0.6$ mL, $V_G/V_0 \cong 0.50$), and C) 0.8 min ($V_G = 0.4$ mL, $V_G/V_0 \cong 0.33$).

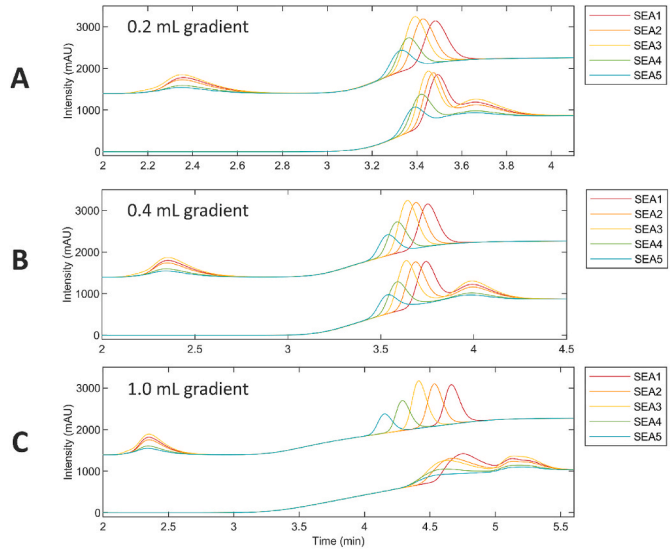

Fig. 4. RPLC (top traces) and gSEC (bottom traces) of S/EA copolymers on the Rapid Resolution SB C18 column (100 × 4.6 mm, 300 Å). Bulk copolymer compositions of S/EA1: 80/20, S/EA2: 73/27, S/EA3: 61/39, S/EA4: 53/47 and S/EA5: 40/60). Gradients from 0 to 60% THF in ACN in A) 0.4 min ($V_G = 0.2$ mL, $V_G/V_0 \cong 0.16$), B) 0.8 min ($V_G = 0.4$ mL, $V_G/V_0 \cong 0.33$), and C) 2.0 min ($V_G = 1.0$ mL, $V_G/V_0 \cong 0.83$); flowrate 0.5 mL•min^{-1}; UV absorbance detection at 210 nm, Column oven temperature set to 25 °C.

reach their critical composition (expected $\varphi_{\text{crit,PMMA}} \approx 0.09 - 0.10$ *vs.* $\varphi_{\text{crit,PS}} \approx 0.5$), even a SEC-gradient that occupied only 33% of the column volume (Fig. 3-C) was not sufficiently steep to eliminate the molecular-weight dependence. Only the three largest PMMA standards eluted nearly unaffected by their molecular weight, *i.e.* close to $\varphi_{\text{crit,PMMA}}$. The smallest PMMA standards eluted unretained (at $t = t_0 + t_G$) in all cases. Equivalent experiments were also performed using RPLC (Fig. 3, filled markers). In this case, the same gradient steepnesses are found to consistently lead to a smaller influence of the molecular weight, as compared with gSEC. We envisage three possible reasons. *i*) Fundamentally, in gSEC analytes need to catch up with the gradient front, and the main mechanism contributing to a higher migration velocity is the extent of exclusion from the pores. The largest possible difference in velocities is about a factor of two, which is only achieved in strong solvents. In contrast, in a conventional gradient experiment the difference in migration velocity between the analytes and the gradient front relies on interaction (adsorption, partition) effects, allowing for an "infinite" ratio of velocities. *ii*) Exclusion effects are strongly reduced in the vicinity of the critical composition (see Fig. 1 and the accompanying discussion). This implies that before the analyte polymers arrive at their appropriate position in the gradient (at $\varphi = \varphi_{\text{crit}}$) their progression slows down. *iii*) For analytes for which $\varphi_{\text{final}} \gg \varphi_{\text{crit}}$, *e.g.* PMMA, the analytes need to cover a wide range of mobile-phase composition. The final composition of the gradient is determined by the last-eluting analytes, in this case PS. Hence, the first-eluting analytes must travel the furthest in the least amount of time.

4.4. 1D-LC separations of S/EA copolymers by RPLC and gSEC

An important advantage of gSEC is that injection occurs in a strong solvent and that breakthrough can be avoided. To evaluate this, one- and two-dimensional separations (SEC × RPLC and SEC × gSEC) of S/EA copolymers were performed. Representative results of the 1D-LC RPLC and gSEC experiments performed on the Zorbax 300 Å column are shown in Fig. 4.

All copolymers have high molecular weights (>70 kDa), so that molecular-weight-independent elution can be expected in RPLC gradients. For RPLC (Fig. 4, upper traces in each frame), the separation based on chemical composition improves when progressively less-steep gradients are used (Fig. 4-A to C). When the gradient is steep enough to allow for a copolymer to elute at their (approximate) critical composition, the chromatographic peak gives an adequate impression of the chemical-composition distribution. At this point, even steeper gradients will result in a reduced selectivity. The optimal gradient will be based on the lowest molecular-weight fraction in the sample. Low-molecular-weight analytes will elute closer to the critical composition when steeper gradients are applied. Therefore, a relatively straightforward method to estimate the required gradient steepness for a sample that features an unknown CCD and MWD will be to perform several gradient experiments and to find the gradient steepness that minimizes the change in peak fronting.

For gSEC (Fig. 4, bottom traces in each frame), the results are different, since in this case the analytes cannot reach their adsorption threshold before eluting from the column, so elution is dominated by molecular weight rather than chemical composition. Such a molecular-weight-dependent elution results in very broad peaks (Fig. 4-C). The highest chemical-composition selectivity can be achieved with gradients that are just steep enough to suppress the molecular-weight effect on elution. For RPLC, a (much) lower gradient steepness suffices. Consequently, RPLC offers greater chemical-composition selectivity than gSEC, when using the 300 Å column. Smaller pore packings might provide improved gSEC separations but will likely lead to reduced recovery and a skewed view of the CCD. The best separation is achieved with the 2-min gradient in RPLC (upper traces in Fig. 4-C).

4.5. SEC × RPLC and SEC × gSEC separations of S/MMA copolymers

One possible attractive application of gSEC is as a second-dimension separation in a 2D-LC system, where SEC is used in the first dimension using a mobile phase that is a very strong solvent in the second dimension. In case of SEC × RPLC, breakthrough may be an issue. Circumvention would require an additional modulation step, *e.g.* by dilution of the transferred fractions with weak solvent before re-injection in the second dimension. A separation of five different S/MMA copolymers, and a homopolymer PS, was performed using SEC × RPLC and SEC × gSEC. The results of these experiments are provided in Fig. 5.

In both cases, a separation based on both the CCD and the MWD is achieved within approximately 35 min. To perform SEC × gSEC (Fig. 5-B), the gradient was delayed to ensure that injection occurred just after the gradient. This resulted in an offset in the second dimension, which was corrected for in Fig. 5-B to allow for easier comparison. After

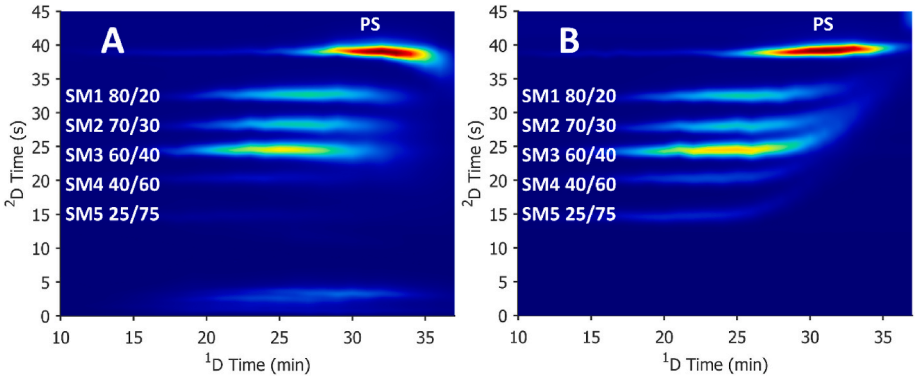

Fig. 5. A) SEC × RPLC and B) SEC × gSEC separation of five S/MMA copolymers and a PS homopolymer. First dimension: SEC; two 150 × 2.1 mm APC SEC columns (2.5-μm particles, 450 Å pore size), mobile phase 100% THF; flowrate 15 μL min^{-1}. Second dimension: A) RPLC or B) gSEC; two 50 × 4.6 mm XBridge BEH Shield RP18 XP columns (3.5-μm particles, 130 Å pore size), flowrate 0.9 mL•min^{-1}. Column oven temperature of both the first and second dimension was set to 25 °C.

correction, the elution composition of the different copolymers and the PS standard are nearly equivalent. Some molecular-weight influence is observed in SEC × gSEC as seen from the upward curving of the elution profiles towards the right in Fig. 5-B. When using RPLC as the second dimension (Fig. 5-A), some breakthrough is observed around 3 min. This results in lower signals for the more-polar copolymers that contain a greater fraction of MMA (SM4 and SM5; signals with 2D retention times of about 20 and 15 min, respectively). Breakthrough is absent in SEC × gSEC (Fig. 5-B). However, due to the molecular-weight effect, SEC × gSEC is not fully orthogonal and careful calibration will be required to obtain quantitative MWD × CCD information.

5. Conclusion

In this work, the applicability of gSEC is investigated for the analysis of the CCD, as an alternative to conventional gradient-elution RPLC. It was shown that gSEC can be advantageous, as it is not susceptible to the breakthrough phenomenon commonly observed in RPLC. For both gradient-elution RPLC and gSEC the application of steep gradients resulted in a reduced influence of the MWD on the separation. Hence, a better impression of the CCD of copolymers could be obtained in such gradients. However, molecular-weight-independent elution was shown to be much more challenging to achieve in gSEC. Because the difference in migration velocity in gSEC is restricted to approximately a factor of two (*i.e.* total exclusion *vs.* total permeation for very large and very small analytes, respectively), it takes long for (relatively) low-molecular-weight analytes to reach their final position in the gradient, which is around their critical composition. This problem is aggravated by a limited choice of columns, as the small pore-size packings that should ideally be used resulted in reduced recovery. This is important to consider for the quantitation of polymers that feature broad molecular-weight distributions since the reduction in recovery seemed to depend on the pore size of the packing relative to the hydrodynamic volume of the polymer. Molecular-weight information and chemical-composition information are likely to be confounded in gSEC. We also implemented gSEC as a second-dimension separation technique for comprehensive LC × LC characterization of polymers. Comprehensive two-dimensional distributions (MWD × CCD) could be obtained by SEC × RPLC, as well as by SEC × gSEC. In the latter case breakthrough in the second dimension was avoided. However, in SEC × gSEC the residual molecular-weight dependence complicates quantitative analysis.

CRediT authorship contribution statement

Leon E. Niezen: Conceptualization, Methodology, Formal analysis, Investigation, Writing – original draft, Visualization. **Jordy D. Kruijswijk:** Conceptualization, Methodology, Formal analysis, Investigation, Writing – review & editing, Visualization. **Gerben B. van Henten:** Conceptualization, Methodology, Formal analysis, Investigation, Writing – review & editing, Visualization. **Bob W.J. Pirok:** Resources, Supervision, Funding acquisition, Project administration, Writing – review & editing. **Bastiaan B.P. Staal:** Methodology, Writing – review & editing, Resources, Supervision. **Wolfgang Radke:** Conceptualization, Methodology, Writing – review & editing. **Harry J.A. Philipsen:** Resources, Project administration, Writing – review & editing. **Govert W. Somsen:** Funding acquisition, Project administration, Writing – review & editing. **Peter J. Schoenmakers:** Resources, Supervision, Funding acquisition, Project administration, Writing – review & editing.

Declaration of competing interest

The authors declare that they have no known competing financial interests or personal relationships that could have appeared to influence the work reported in this paper.

Data availability

Data will be made available on request.

Acknowledgements

This research was performed within the UNMATCHED project, which is supported by BASF, DSM and Nouryon and receives funding from the Dutch Research Council (NWO) in the framework of the Innovation Fund for Chemistry (CHIPP Project 731.017.303) and from the Ministry of Economic Affairs in the framework of the "TKI-toeslagregeling". BP acknowledges Agilent (UR grant #4354).

LN, JK, GH and BP are part of the Chemometrics and Advanced Separations Team (CAST) within the Centre for Analytical Sciences Amsterdam (CASA). The valuable contributions of the CAST members are gratefully acknowledged.

Appendix A. Supplementary data

Supplementary data to this article can be found online at https://doi.org/10.1016/j.aca.2023.341041.

References

[1] A.M. Striegel, Multiple detection in size-exclusion chromatography of macromolecules, Anal. Chem. 77 (2005), https://doi.org/10.1021/ac053345e.

[2] W.C. Knol, T. Gruendling, P.J. Schoenmakers, B.W.J. Pirok, R.A.H. Peters, Co-Polymer sequence determination over the molar mass distribution by size-exclusion chromatography combined with pyrolysis - gas chromatography, J. Chromatogr. A 1670 (2022), 462973, https://doi.org/10.1016/j.chroma.2022.462973.

[3] H.W. Siesler, Infrared spectroscopy of polymers, Appl. Spectrosc. Rev. 11 (1976), https://doi.org/10.1080/05704927608081704.
[4] J.F. Kennedy, A.D. Suett, NMR spectroscopy of polymers, Carbohydr. Polym. 27 (1995), https://doi.org/10.1016/0144-8617(95)90065-9.
[5] T. Górecki, J. Poerschmann, In-column pyrolysis: a new approach to an old problem, Anal. Chem. 73 (2001) 2012–2017, https://doi.org/10.1021/ac000913b.
[6] E. Kaal, H.G. Janssen, Extending the molecular application range of gas chromatography, J. Chromatogr. A 1184 (2008) 43–60, https://doi.org/10.1016/j.chroma.2007.11.114.
[7] P. Schoenmakers, P. Aarnoutse, Multi-dimensional separations of polymers, Anal. Chem. 86 (2014) 6172–6179, https://doi.org/10.1021/ac301162b.
[8] H.J.A. Philipsen, Determination of chemical composition distributions in synthetic polymers, J. Chromatogr. A 1037 (2004) 329–350, https://doi.org/10.1016/j.chroma.2003.12.047.
[9] G. Glöckner, Gradient HPLC of Copolymers and Chromatographic Cross-Fractionation, 1991, https://doi.org/10.1007/978-3-642-75799-0.
[10] G. Glöckner, H.G. Barth, Use of high-performance liquid chromatography for the characterization of synthetic copolymers, J. Chromatogr. A 499 (1990), https://doi.org/10.1016/S0021-9673(00)97009-2.
[11] G. Glöckner, J.H.M. van den Berg, Copolymer fractionation by gradient high-performance liquid chromatography, J. Chromatogr. A 384 (1987), https://doi.org/10.1016/S0021-9673(01)94665-5.
[12] G. Glöckner, High-performance precipitation liquid chromatography, Trends Anal. Chem. 4 (1985), https://doi.org/10.1016/0165-9936(85)87062-X.
[13] E. Uliyanchenko, Size-exclusion chromatography - from high-performance to ultra-performance, Anal. Bioanal. Chem. 406 (2014) 6087–6094, https://doi.org/10.1007/s00216-014-8041-z.
[14] S.T. Popovici, P.J. Schoenmakers, Fast size-exclusion chromatography - theoretical and practical considerations, J. Chromatogr. A 1099 (2005), https://doi.org/10.1016/j.chroma.2005.08.071.
[15] A.M. Striegel, Method development in interaction polymer chromatography, TrAC, Trends Anal. Chem. 130 (2020), https://doi.org/10.1016/j.trac.2020.115990.
[16] W. Radke, Polymer separations by liquid interaction chromatography: principles - prospects - limitations, J. Chromatogr. A 1335 (2014) 62–79, https://doi.org/10.1016/j.chroma.2013.12.010.
[17] E.F. Casassa, Remarks on light scattering from polymers in mixed solvents: effects of polymer molecular weight, molecular weight distribution, and solvent composition, Polym. J. 3 (1972) 517–525, https://doi.org/10.1295/polymj.3.517.
[18] R. Mhatre, I.S. Krull, Determination of on-line differential refractive index and molecular weight via gradient HPLC interfaced with low-angle laser light scattering, ultraviolet, and refractive index detection, Anal. Chem. 65 (1993) 283–286, https://doi.org/10.1021/ac00051a016.
[19] A.M. Striegel, P. Sinha, Absolute molar mass determination in mixed solvents. 1. Solving for the SEC/MALS/DRI "trivial" case, Anal. Chim. Acta 1053 (2019) 186–195, https://doi.org/10.1016/j.aca.2018.11.051.
[20] K.J. Bombaugh, R.N. King, A.J. Cohen, A new gradient elution chromatograph, J. Chromatogr. A 43 (1969) 332–338, https://doi.org/10.1016/s0021-9673(00)99209-4.
[21] H.J.A. Philipsen, M. Oestreich, B. Klumperman, A.L. German, Characterization of low-molar-mass polymers by gradient polymer elution chromatography. III. Behaviour of crystalline polyesters under reversed-phase conditions, J. Chromatogr. A 775 (1997), https://doi.org/10.1016/S0021-9673(97)00208-2.
[22] X. Jiang, A. van der Horst, P.J. Schoenmakers, Breakthrough of polymers in interactive liquid chromatography, J. Chromatogr. A 982 (2002) 55–68, https://doi.org/10.1016/S0021-9673(02)01483-8.
[23] Y. Mengerink, R. Peters, M. Kerkhoff, J. Hellenbrand, H. Omloo, J. Andrien, M. Vestjens, S. van der Wal, Analysis of linear and cyclic oligomers in polyamide-6 without sample preparation by liquid chromatography using the sandwich injection method. I. Injection procedure and column stability, J. Chromatogr. A 876 (2000) 37–50, https://doi.org/10.1016/S0021-9673(00)00179-5.
[24] E. Reingruber, F. Bedani, W. Buchberger, P. Schoenmakers, Alternative sample-introduction technique to avoid breakthrough in gradient-elution liquid chromatography of polymers, J. Chromatogr. A 1217 (2010) 6595–6598, https://doi.org/10.1016/j.chroma.2010.07.073.
[25] D. Berek, Liquid chromatography of macromolecules under limiting conditions of desorption. 1. Principles of the method, Macromolecules 31 (1998) 8517–8521, https://doi.org/10.1021/ma980533g.
[26] D. Berek, Separation of parent homopolymers from diblock copolymers by liquid chromatography under limiting conditions desorption, 1 - principle of the method, Macromol. Chem. Phys. 209 (2008) 695–706, https://doi.org/10.1002/macp.200700540.
[27] M. Schollenberger, W. Radke, SEC-Gradients, an alternative approach to polymer gradient chromatography: 1. Proof of the concept, Polymer (Guildf). 52 (2011) 3259–3262, https://doi.org/10.1016/j.polymer.2011.05.047.
[28] M. Schollenberger, W. Radke, Size exclusion chromatography-gradients, an alternative approach to polymer gradient chromatography: 2. Separation of poly (meth)acrylates using a size exclusion chromatography-solvent/non-solvent gradient, J. Chromatogr. A 1218 (2011) 7827–7831, https://doi.org/10.1016/j.chroma.2011.08.090.
[29] H. Maier, F. Malz, W. Radke, Characterization of the chemical composition distribution of poly(n -butyl acrylate-stat-acrylic acid)s, Macromol. Chem. Phys. 216 (2015) 228–234, https://doi.org/10.1002/macp.201400399.
[30] H. Maier, F. Malz, G. Reinhold, W. Radke, SEC gradients: an alternative approach to polymer gradient chromatography. Separation of poly(methyl methacrylate-stat-methacrylic acid) by chemical composition, Macromolecules 46 (2013) 1119–1123, https://doi.org/10.1021/ma3023553.
[31] G. Glöckner, D. Wolf, H. Engelhardt, Separation of copoly(styrene/acrylonitrile) samples according to composition under reversed phase conditions, Chromatographia 32 (1991) 107–112, https://doi.org/10.1007/BF02325011.
[32] L.R. Snyder, M.A. Stadalius, M.A. Quarry, L.R. Snyder, Gradient elution in reversed-phase HPLC separation of macromolecules, Anal. Chem. 55 (1983) 1412A–1430A, https://doi.org/10.1021/ac00264a001.
[33] P. Schoenmakers, F. Fitzpatrick, R. Grothey, Predicting the behaviour of polydisperse polymers in liquid chromatography under isocratic and gradient conditions, J. Chromatogr. A 965 (2002) 93–107, https://doi.org/10.1016/S0021-9673(01)01322-X.
[34] F. Fitzpatrick, R. Edam, P. Schoenmakers, Application of the reversed-phase liquid chromatographic model to describe the retention behaviour of polydisperse macromolecules in gradient and isocratic liquid chromatography, J. Chromatogr. A 988 (2003) 53–67, https://doi.org/10.1016/S0021-9673(02)02050-2.
[35] L.R. Snyder, Linear elution adsorption chromatography. VII. gradient elution theory, J. Chromatogr. A 13 (1964) 415–434, https://doi.org/10.1016/s0021-9673(01)95138-6.
[36] L.R. Snyder, J.W. Dolan, High-Performance Gradient Elution: the Practical Application of the Linear-Solvent-Strength Model, 2006, https://doi.org/10.1002/0470055529.
[37] L.E. Niezen, B.B.P. Staal, C. Lang, H.J.A. Philipsen, B.W.J. Pirok, G.W. Somsen, P. J. Schoenmakers, Recycling gradient-elution liquid chromatography for the analysis of chemical-composition distributions of polymers, J. Chromatogr. A 1679 (2022), 463386, https://doi.org/10.1016/J.CHROMA.2022.463386.
[38] M. van Hulst, A. van der Horst, W.T. Kok, P.J. Schoenmakers, Comprehensive 2-D chromatography of random and block methacrylate copolymers, J. Separ. Sci. 33 (2010) 1414–1420, https://doi.org/10.1002/jssc.200900737.
[39] X. Jiang, A. van der Horst, V. Lima, P.J. Schoenmakers, Comprehensive two-dimensional liquid chromatography for the characterization of functional acrylate polymers, J. Chromatogr. A 1076 (2005) 51–61, https://doi.org/10.1016/j.chroma.2005.03.135.
[40] S.M. Graef, A.J.P. van Zyl, R.D. Sanderson, B. Klumperman, H. Pasch, Use of gradient, critical, and two-dimensional chromatography in the analysis of styrene- and methyl methacrylate-grafted epoxidized natural rubber, J. Appl. Polym. Sci. 88 (2003) 2530–2538, https://doi.org/10.1002/app.12060.
[41] M.I. Malik, Critical parameters of liquid chromatography at critical conditions in context of poloxamers: pore diameter, mobile phase composition, temperature and gradients, J. Chromatogr. A 1609 (2020), https://doi.org/10.1016/j.chroma.2019.460440.
[42] Y. Brun, P. Alden, Gradient separation of polymers at critical point of adsorption, J. Chromatogr. A 966 (2002) 25–40, https://doi.org/10.1016/S0021-9673(02)00705-7.
[43] Y. Brun, P. Foster, Characterization of synthetic copolymers by interaction polymer chromatography: separation by microstructure, J. Separ. Sci. 33 (2010) 3501–3510, https://doi.org/10.1002/jssc.201000572.
[44] A.M. Caltabiano, J.P. Foley, A.M. Striegel, Organic solvent modifier and temperature effects in non-aqueous size-exclusion chromatography on reversed-phase columns, J. Chromatogr. A 1531 (2018) 83–103, https://doi.org/10.1016/j.chroma.2017.11.027.
[45] A.P. Schellinger, D.R. Stoll, P.W. Carr, High speed gradient elution reversed-phase liquid chromatography, J. Chromatogr. A 1064 (2005) 143–156, https://doi.org/10.1016/j.chroma.2004.12.017.